

Optical Engineering

OpticalEngineering.SPIEDigitalLibrary.org

Ten-year summary of the Boulder Damage Symposium annual thin film laser damage competition

Christopher J. Stolz
Raluca A. Negres

Ten-year summary of the Boulder Damage Symposium annual thin film laser damage competition

Christopher J. Stolz* and Raluca A. Negres

Lawrence Livermore National Laboratory, Livermore, California, United States

Abstract. The thin film damage competition series at the Boulder Damage Symposium provides an opportunity to observe general trends in laser damage behavior between different coating types (high reflector, antireflector, polarizer, and Fabry–Perot filter), wavelength ranges (193 to 1064 nm), and pulse length ranges (40 fs to 18 ns). Additionally, the impact of deposition process, coating material, cleaning process, and layer count can be studied within a single year or more broadly across the history of this competition. Although there are instances where participants attempted to isolate a single variable to better understand its impact on laser resistance, this series of competitions isolates the variable of the damage testing service and protocol for a wide variety of participants to enable the observation of general trends. In total, 275 samples from 58 different participants have been tested at four different laser damage testing facilities over the last 10 years. Hafnia was clearly the best high refractive index material except for ultraviolet (UV) applications, although a wide range of high refractive index materials performed well. The best deposition process varied significantly between the different competitions. The best deposition process was dependent on the coating type, wavelength, and pulse duration. For 1064-nm coatings with nanosecond scale pulse lengths, e-beam coatings tended to be the best performers. For short-pulse length NIR mirrors and nanosecond pulse length UV mirrors, densified coating processes, which all involved sputtering of the target material, were the best performers. For UV antireflector (AR) coatings and excimer mirrors, both tested at nanosecond pulse lengths, they tended to favor very low energetic deposition methods yielding soft coatings, such as sol gel dip coating for the AR and resistive heating of fluorides for the excimer mirrors. Finally, cleaning method and layer count had a less obvious correlation with laser resistance over the history of this thin film damage competition series. © 2018 Society of Photo-Optical Instrumentation Engineers (SPIE) [DOI: [10.1117/1.OE.57.12.121910](https://doi.org/10.1117/1.OE.57.12.121910)]

Keywords: laser damage testing; mirror; antireflector; Fabry–Perot filter; polarizer; thin film; multilayer; excimer laser; femtosecond laser; nanosecond laser; near infrared laser; ultraviolet laser; ISO21254-2.

Paper 181015SS received Jul. 16, 2018; accepted for publication Nov. 19, 2018; published online Dec. 18, 2018.

1 Introduction

In 2008, a thin film laser damage competition was launched at the Boulder Damage Symposium (BDS).¹ A total of 275 samples have been tested with submissions from 58 different participants listed in Table 1 representing seven different countries, as illustrated in Fig. 1. Nearly, half of the participants came from the USA, one third came from Europe, and almost one fifth came from Asia. The participants included commercial coating vendors, universities, and research institutes. Only one participant, Laser Zentrum Hannover (LZH), participated in all 10 competitions.

The participants provided samples at no cost to the competition. At the beginning of this series of competitions, some of the participants declined to provide some of the basic process details, such as high refractive index material and deposition process. After a few years, it was decided that the following information would be mandatory to participate in the competition so that some general trends could be ascertained from the competition and shared at the symposium:

- Deposition process
- Coating materials
- Number of layers
- Substrate material

- Cleaning method
- Spectral performance

Over the history of this competition, four different coating types [highreflector (HR), antireflector (AR), Fabry–Perot filter, and polarizer] have been tested over a wavelength range of 193 to 1064 nm and pulse length range of 40 fs to 18 ns, as summarized in Table 2.^{1–10} Four different damage testing facilities, including Spica (four competitions), LZH (two competitions), Quantel (two competitions), and the Ohio State University (OSU; two competitions) graciously donated their testing services to this series of competitions.

There were several motivations for this thin film damage competition. First, summaries of the requested process data would undoubtedly create opportunities for the laser damage community not only to learn the current performance status of high damage threshold thin films, but also to learn from the general trends of the competition. Second, the anonymity of the reported results would provide companies a safe way to evaluate how their high fluence thin film technology ranked against the other participants and hopefully promote process improvements. Finally, this competition was hoped to reverse a 20-year decline in the number of thin film papers submitted to the SPIE Laser Damage Conference. Although there are many factors that impact paper submissions to conferences, there is a positive resurgence in thin film papers

*Address all correspondence to Christopher J. Stolz, E-mail: stolz1@llnl.gov

Table 1 Participant list for the annual BDS thin film damage competition.

Company	Country	2008	2009	2010	2011	2012	2013	2014	2015	2016	2017	Total
Absolute Coatings	USA			X								1
Advanced Thin Films	USA	X	X						X	X		4
Aerospace Times Laser	China								X	X		2
Agilent Technology	USA	X										1
Alpine Research Optics	USA										X	1
Altechna Co Ltd.	Lithuania				X							1
Arrow Thin Films	USA			X					X	X		3
Berliner Glas KGaA	Germany	X										1
Carl Zeiss	Germany								X	X		2
Center for Physical S&T	Lithuania										X	1
Changchuan Inst. of Optics	China					X	X					2
Colorado State University	USA								X	X		2
Corning	USA				X							1
Cutting Edge Coatings	Germany										X	1
CVI Melles Griot	UK					X	X					2
CVI Melles Griot	USA					X	X		X	X	X	5
FiveNine Optics	USA										X	1
Fraunhofer Institute	Germany		X									1
G&H, CCI	USA			X								1
G&H, General Optics	USA			X								1
G&H, Ilminster	UK		X	X								2
Hardin Optical Company	USA					X	X					2
Infinite Optics	USA										X	1
Institute of Optics & Electr.	China	X	X									2
Jenoptik Laser	Germany		X									1
Jiutle	China			X								1
Kugler	Germany	X										1
Laser Components	Germany	X	X			X	X	X	X	X	X	8
LZH	Germany	X	X	X	X	X	X	X	X	X	X	10
Laserhof Frielingen	Germany	X				X	X				X	4
LaserOptik	Germany	X				X	X					3
LLNL	USA			X								1
Layertec Optical Coatings	Germany		X	X							X	3
Nikon	Japan	X	X	X	X				X	X	X	7
Okamoto Optics Work	Japan		X			X	X			X		4
Optical Coatings Japan	Japan			X					X	X		3

Table 1 (Continued).

Company	Country	2008	2009	2010	2011	2012	2013	2014	2015	2016	2017	Total
Optida UAB	Lithuania	X							X	X		3
Optimax Systems	USA					X	X					2
Opturn Company Ltd.	China					X	X					2
Photonics Products Group	USA	X										1
Plymouth Gratings	USA	X										1
Precision Photonics Corp.	USA		X									1
Quality Thin Films	USA	X	X								X	3
Research Electro-Optics	USA								X	X	X	3
RhySearch	Switzerland										X	1
Sandia National Lab	USA					X	X		X	X		4
Schott	Switzerland					X	X		X	X		4
Schott	USA		X									2
SIOM	China	X	X		X	X	X					5
Shichuan Dorder Technology	China					X	X					2
SLS Optics	UK				X	X	X		X	X	X	6
Spectra-Physics	USA		X									1
TelAztec	USA	X									X	2
Tongji University	China						X	X	X	X	X	5
Twin Star Optics	USA	X										1
U of R, LLE	USA	X									X	2
VLOC	USA	X										1
Zygo	USA								X	X		2
Total	58	29	15	11	6	17	17	3	17	18	18	

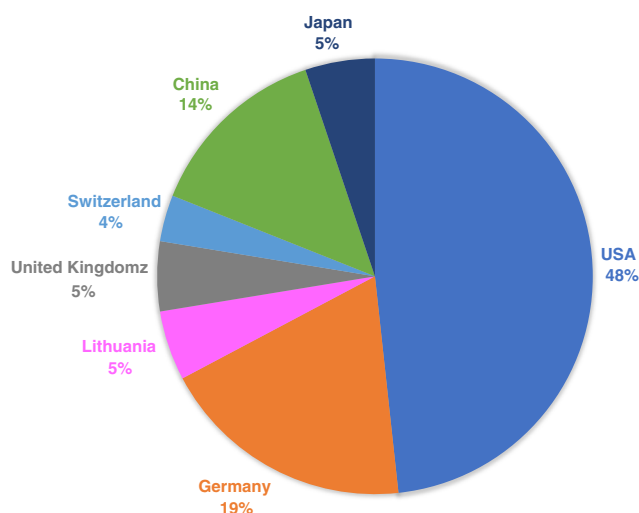


Fig. 1 Distribution of participants by country.

since the thin film damage competition started, as observed in Fig. 2.

2 Samples

The substrates for this series of competitions were all provided by the participants. The damage test sample diameter and thickness were standardized, and all the samples were put into identical polyethylene terephthalate (PETG) plastic containers to maintain test sample anonymity. A unique participant code consisting of a letter and a number series was assigned to each participant's sample. For example, A-1 and A-2 would be a typical code for a participant that contributed two samples. To make this a double-blind competition, a nontechnical administrative assistant maintained a spreadsheet that mapped the participant name to the participant code. The competition organizer and the damage testing service were provided only the participant code with the participant-supplied performance data for each test sample. At the completion of the damage testing, each participant was

Table 2 Coating specifications and performance summary.

Parameter	Year										
	2008	2009	2010	2011	2012	2013	2014	2015	2016	2017	
Coating type	HR	HR	AR	HR	Polarizer	Polarizer	Fabry-Perot	HR	HR	HR	
Wavelength (nm)	1064	786	355	193	1064	1064	1064	773 ± 50	773 ± 50	773 ± 50	355
Pulse length (ns)	5	0.00018	7.5	13	10	10	3.5 and 18	0.15	0.00004	0.00004	5
Repetition rate (Hz)	10	1000	10	100	20	20	10	500	500	500	10
Reflectivity (%)	>99.5	>99.5	>99.5	>97	>99	>99	>99	>99.5	>99.5	>99.5	>99.5
Transmission (%)			>99.75		>95		>90				
Polarization					P	S	P	P	P	P	P
Incident angle (deg)	0	0	0	0	56.4	56.4	10-30	45	45	45	45
GDD (fs ²)								100	100	100	
Testing service	Spica	LZH	Spica	LZH	Spica	Quantel	Quantel	OSU	OSU	OSU	Spica
Test methodology	Raster	ISO	Raster	ISO	ISO	ISO	Raster	Raster	Raster	Raster	Raster
No. of participants	19	15	11	6	17	17	3	17	18	18	18
No. of samples	35	27	29	12	26	31	5	33	42	42	35
Best high refractive index material	Unknown	HfO ₂	None	LaF ₃	HfO ₂	HfO ₂	HfO ₂	HfO ₂	HfO ₂ & Nb ₂ O ₅	HfO ₂	Al ₂ O ₃
Best low refractive index material	SiO ₂	SiO ₂	SiO ₂	AlF ₃ & MgF ₂	SiO ₂	SiO ₂	SiO ₂	SiO ₂	SiO ₂	SiO ₂	SiO ₂
Best deposition process	e-beam	Sputtering O ₂ enhanced	Sol gel	RH	e-beam	IAD	e-beam	IBS	Magnetron sputtering	IBS	IBS
"Honorable mention" high refractive index materials	Ta ₂ O ₅	TiO ₂ ; ZrO ₂	HfO ₂ and SiO ₂ (mix)	GdF ₃	Ta ₂ O ₅ & HfO ₂ ; ZrO ₂	HfO ₂ ; ZrO ₂ ; ZrO ₂ and Nb ₂ O ₅ ; HfO ₂ and ZrO ₂	HfO ₂				
"Honorable mention" deposition processes	IAD; IBS	Magnetron sputtering; e-beam; IBS; sputtering	Magnetron sputtering; e-beam	e-beam	IAD	e-beam	e-beam	IAD; e-beam	IBS; IAD	IBS; IAD	e-beam; magnetron sputtering
Highest laser resistance (J/cm ²)	130	1.1	48	1.9	36	43	22 and 25	9	0.9	0.9	14

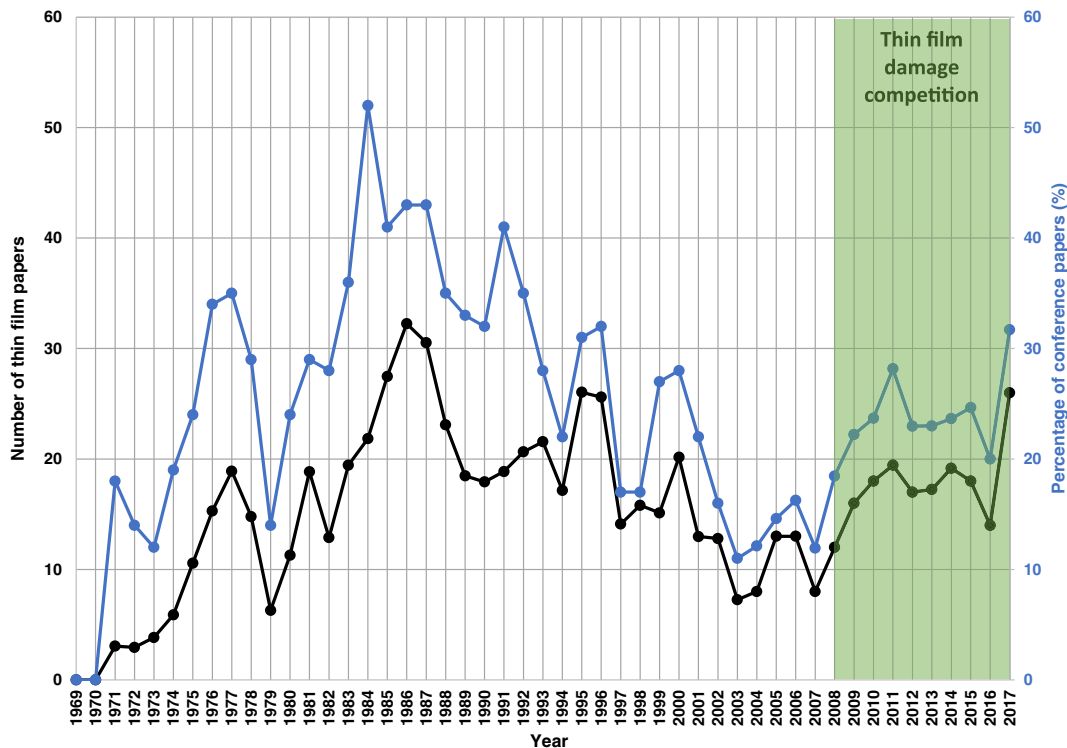


Fig. 2 History of thin film papers presented at the Laser Damage Conference.

informed of their unique vendor code and their laser damage threshold result. A summary of the results was presented at the SPIE Laser Damage Conference, and the written summaries are in the conference proceedings.¹⁻¹⁰ The advantage of a double-blind competition is that participants could submit samples without concern about advertising a poor result, particularly for the commercial participants. This competition anonymity also prevented advertisement for the participant with the best performing test sample.

Specifications for the 10 competitions are listed in Table 2. In addition, the environmental requirements were ambient lab conditions (40% relative humidity and 20°C). There were no coating stress or reflected wavefront requirements. Each participant provided spectral data to validate spectral performance. Participants also provided a brief description of the coating deposition process, coating materials, and the layer count.

For two of the competitions, the Brewster angle polarizer of 2012 and 2013 and the broadband short-pulse high reflector of 2015 and 2016, the same samples were tested in both years to understand the impact of polarization and pulse length, respectively. Also, in 2014, the Fabry-Perot coatings were damage tested at two different pulse lengths. For all other years, the samples were only damage tested under a single set of conditions.

3 Damage Testing

Damage testing for each year of this competition was performed at one of four different laser damage testing services, Spica Technologies,¹¹ LZH,¹² Quantel Laser,¹³ and the OSU.¹⁴ For the broadband mirrors, the group dispersion delay (GDD) measurements were performed at KMLabs, Inc.¹⁵ These measurements were all graciously donated by these testing services. Damage testing was divided into

two different testing protocols. A 10 mm × 10 mm area raster scanning protocol, as described by Borden et al.,¹⁶ was employed at Spica. A raster scan area of 3 mm × 3 mm was employed at OSU because of a significantly smaller test beam. In both cases, the beam diameter as defined by the 90% intensity was used as the incremental step size between laser pulses in both the x - and y -direction. The ISO 21254-2 test^{17,18} was employed at both LZH and Quantel Laser. The damage testing service and testing protocol are indicated within Table 2.

There are advantages and disadvantages with both laser test protocols. For the ISO test to determine the unconditioned damage threshold, a series of 10 sites are tested at a constant fluence, and then another 10 sites are tested at an elevated fluence; this process is repeated until a damage probability curve is established. From this damage probability curve, a zero-damage probability fluence is calculated. As part of this test, the number of shots per site is defined to determine aging or lifetime. Typically, the outcome of the damage test at a given location is monitored using a scatter and/or plasma detector; in addition, test sites may also be examined before and after irradiation under an optical microscope. To test for laser conditioning, a fluence ramp on each test site is performed.

The raster scan protocol involves scanning a 1 cm × 1 cm area using laser pulses with fixed fluence at 10 Hz or higher repetition rate and a predetermined spatial beam overlap (typically, the sample is stepped in the x - and y -axis by the 90% intensity beam diameter). The 1 cm² area can also be scanned multiple times at progressively higher fluences to construct a damage density curve versus fluence. For example, in the case of the first damage competition in 2008 (a 1064 nm normal incident high reflector tested at 5 ns), the first scan occurred at 1 J/cm² and each

subsequent scan was increased in 3 J/cm² increments. Three categories were defined as follows: “no damage,” “initiation,” and “failed.” “No damage” was defined as the highest fluence at which no visible change occurred to the coating. “Initiation” was the highest fluence at which pinpoints as large as 100 μm were observed; however, none of the pinpoint damage grew upon repeated illumination. “Fail” was defined as the lowest fluence where pinpoint damage exceeded 100 μm, pinpoint damage grew upon repeated illumination or pinpoint damage occurred in more than 1% of the total number of sites. Like the ISO test, scatter and plasma detectors monitor the test surface during the raster test and report laser damage as a function of sample position. Pre- and post-test microscopy are also utilized to diagnose changes in the surface due to laser irradiation.

The fundamental differences in the testing protocol are the raster scan test typically interrogates 20× more sites, so it can be better at determining the laser damage resistance of a coating that is fluence-limited by stochastic defects that have a broad range of damage thresholds and defect densities. However, for coatings that have uniform laser resistance and defect densities, the ISO test determines a much more precise laser damage threshold from the zero-damage extrapolation of the damage probability curve. The raster scan test cannot determine the damage threshold any more precisely than the incremental fluence used during the test. The raster scan protocol does not determine the unconditioned laser damage threshold because of the very nature of scanning the surface with Gaussian spatial beam profiles and incremental steps less than the beam diameter, i.e., nonzero fluence overlap between adjacent sites.¹⁹ For the raster scan

test, coating lifetime can be determined by retesting damage sites at multiple shots to determine their stability. ISO testing has the advantage of determining very subtle laser-induced morphological changes because sample interrogation is done under a high magnification microscopy before and after each laser exposure; however, as scanning optical microscopes and imaging processing software become more commonplace, the difference in these two protocols is becoming less pronounced. More detailed descriptions of the setup and testing protocol can be found in the ISO standard and NIF damage test paper.¹⁶⁻¹⁸

The laser fluence at the sample plane is calibrated prior to damage testing and checked frequently to ensure repeatability of results over time. Most test facilities utilize a beam sampler inserted in the main beam path to provide a reference diagnostic arm, which duplicates the laser beam propagation to an equivalent sample plane. The beam spatial profile (i.e., beam diameter) and energy of this secondary, low energy beam are recorded and calibrated with respect to the primary, high energy beam incident onto the sample. The peak laser fluence in a plane normal to beam propagation is the most common metric for laser damage test results. Shot-to-shot laser fluctuations in both energy and spatial beam characteristics are typical sources of uncertainty in the test laser fluence and amount to ~15% deviations from the nominal values for most laser systems used in these studies.

4 Coating Materials

Over the history of this damage competition, 15 different high refractive materials have been used, as illustrated in Fig. 3. These materials are distributed among five diverse

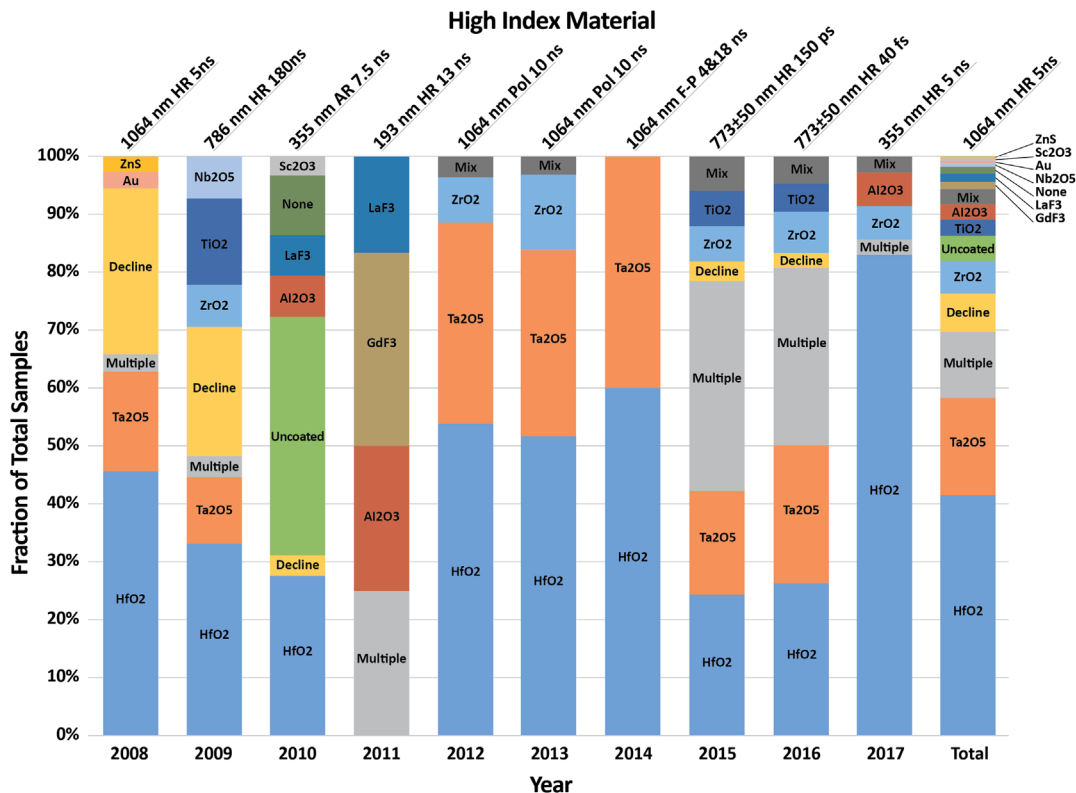


Fig. 3 High refractive index coating material distribution for the 10 thin film damage competitions. In some cases, the participants declined to reveal the composition of the high refractive index material and, in a few other cases, multiple high refractive index materials were used.

types, including metals (Au, Ag, and Cu), metallic oxides (Al_2O_3 , HfO_2 , Nb_2O_5 , Sc_2O_3 , Ta_2O_5 , TiO_2 , and ZrO_2), fluorides (LaF_3 and GdF_3), a sulphide (ZnS), and mixed oxides created by sputtering from a single target fabricated of two materials (HfO_2 and SiO_2 or HfO_2 and Al_2O_3). For the low refractive index materials, illustrated in Fig. 4, there was considerably less diversity consisting of only four different materials, an oxide (SiO_2) and three different metal fluorides (AlF_3 , MgF_2 , and Na_3AlF_6). Most of the test samples had coating designs that consisted of only two materials: a high refractive index material and a low refractive index material. The most frequently used material combination for this series of competitions was HfO_2 and SiO_2 , particularly for coatings centered in the near-infrared spectral region, and at least half of the winning test samples were manufactured with these two materials, as can be seen from Table 2. For coatings in the ultraviolet range of the spectrum, the general trend was to use metallic oxides for the high index material and SiO_2 as the low index material at 355 nm. In the deeper ultraviolet at 193 nm, predominately fluorides were used as both the high and low refractive index material due to their larger bandgap, as illustrated in Fig. 5.

For the excimer mirror competition in 2011 and the broadband short pulse mirrors in the 2015 and 2016 competitions, a considerable number of the coating designs consisted of more than two coating materials. Both coating types used more than two coating materials because of the desire to increase the spectral bandwidth and the GDD for the broadband short pulse mirrors beyond what could be achieved through a quarter-wave stack design of the most

laser resistant high and low refractive index materials. Since the laser damage resistance of coating materials tends to increase with decreasing refractive index, the standard design strategy is to place the lower laser resistant coating materials (which broaden the spectral bandwidth) on the bottom of the coating design where there is a lower electric field and place the high laser resistant coating materials on the top of the coating design where the electric field is highest.

Unsurprisingly, the laser resistance of the samples that contained metallic layers was low. Metallic films were used for the 1064-nm high reflector of 2008 (Au) and for the broadband short pulse mirrors of 2015 and 2016 (Ag and Cu). In the case of the 1064-nm high reflector, the participant supplied a gold (Au) single layer and an enhanced gold coating, which means that the gold layer is typically overcoated with alternating layers of a metallic oxide and silica to improve the reflectivity. The enhanced gold mirror performed better than the single layer. For the broadband short pulse mirrors, the two test samples with metallic layers were likely at the bottom of the coating to increase the bandwidth of the coating. Unfortunately, the coating containing Ag, Cu, HfO_2 , and SiO_2 did not meet the GDD specification due to a 1% centering error. Equally, unsurprisingly, the ZnS coating did not perform well. This material is much better suited to far infrared wavelengths.

The 355-nm antireflection coating of 2010 was the only coating within this competition series where the best performing samples were a single layer. Because sol gel coatings can be extremely porous, the refractive index of

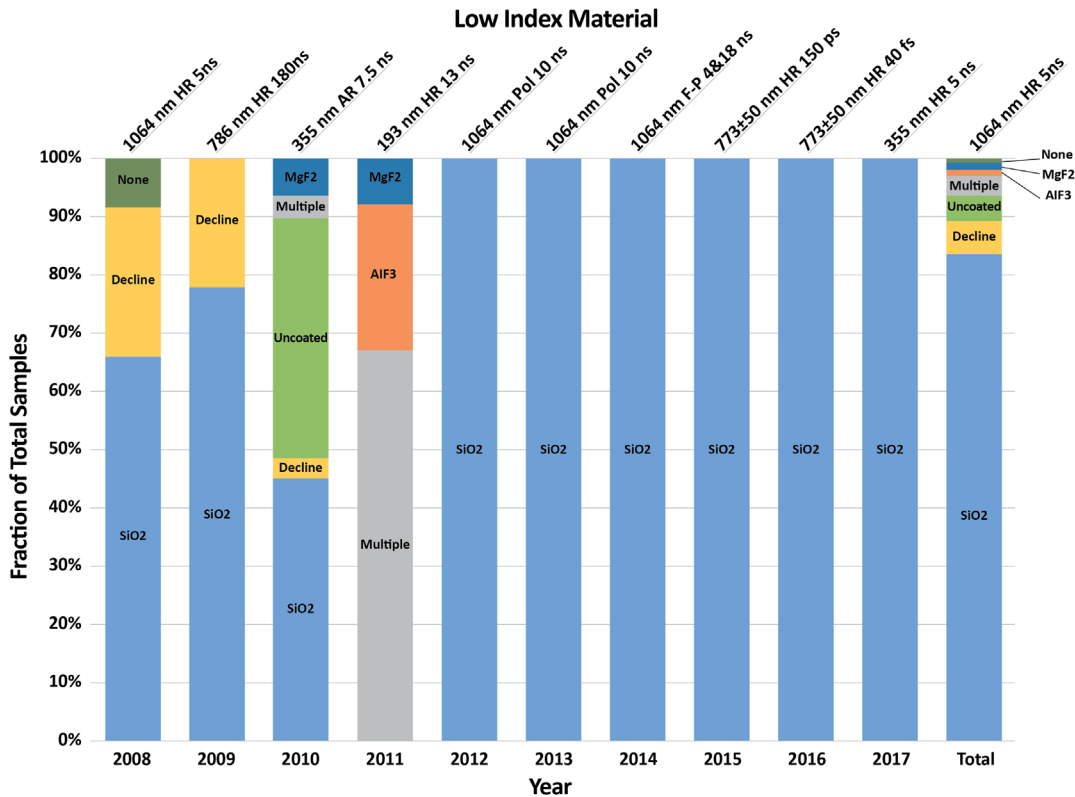


Fig. 4 Low refractive index coating material distribution for the 10 thin film damage competitions. In some cases, the participants declined to reveal the composition of the low refractive index material and, in a few other cases, particularly in 2011, multiple low refractive index materials were used.

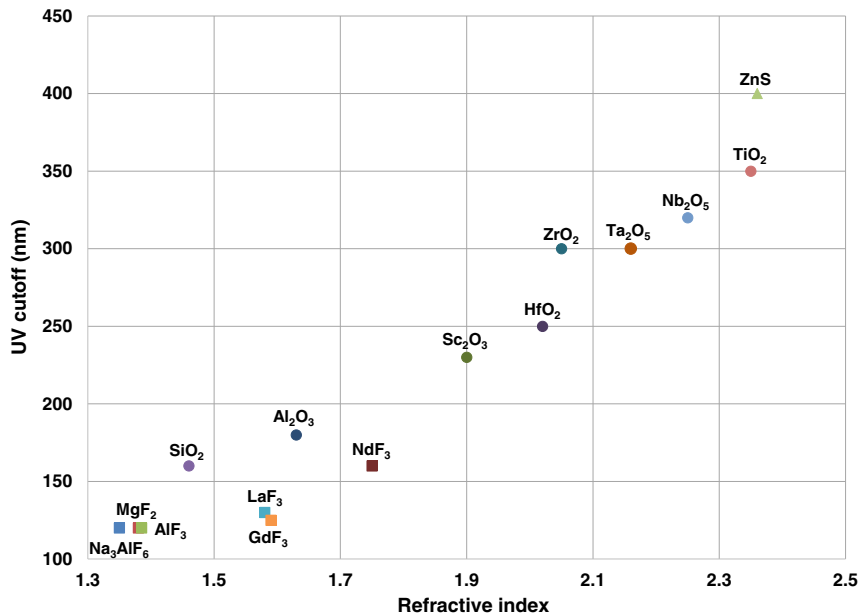


Fig. 5 Refractive index and ultraviolet (UV) cutoff for the 14 different metal oxides (circles), metal fluorides (squares), and a sulfide (triangle) used in the 10 competitions.

a single SiO₂ layer can be lowered to the point of becoming an extremely effective antireflection coating.^{20,21} Other deposition technologies, with the exception of glancing angle deposition²² of which no samples deposited with this process have been submitted to this series of competitions, require a combination of high and low refractive index materials to meet the spectral requirements. In the case of this 355-nm antireflection coating competition, participants also supplied uncoated control samples to gain insight into whether the

substrate finishing^{23,24} or coating limited the laser resistance of the test samples.

5 Coating Deposition Processes

Eight different deposition processes have been used to manufacture test samples for this laser damage competition series, as illustrated in Fig. 6. They are divided into three classes: thermal evaporation [electron-beam (e-beam), electron-beam with ion-assisted deposition (IAD), electron-beam with

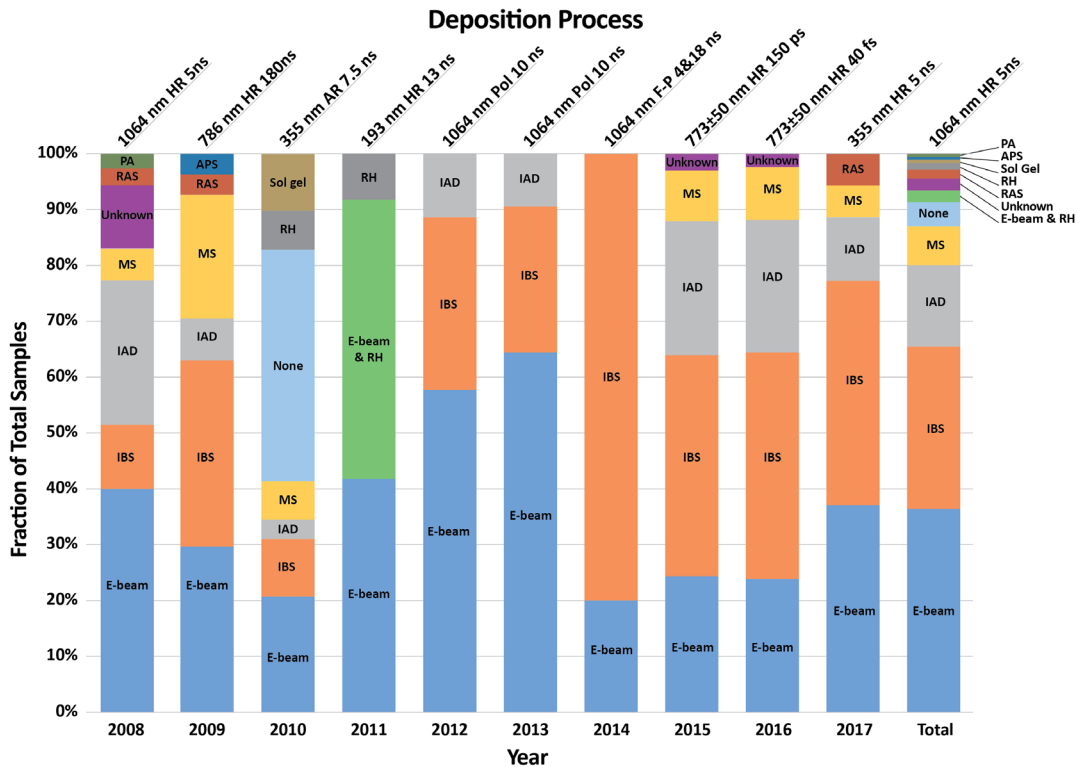


Fig. 6 Deposition process distribution for the 10 thin film damage competitions. In a few cases, the deposition process was not reported by the participants.

plasma assist, and resistive heating (RH)]; sputtering [ion beam sputtering (IBS), magnetron sputtering (MS), radical-assisted sputtering]; and solution deposition (sol gel). The best deposition process was very specific to the individual competitions, as illustrated in Table 2; however, a few general trends emerged. The 1064-nm nanosecond pulse coatings (HR, polarizer, and Fabry–Perot filter) deposited by e-beam or e-beam with IAD²⁵ were the most laser resistant. It has been proposed that the dominant damage mechanism for these coatings is nodule ejection and that e-beam coatings are fragile enough to have benign nodule ejection pits that are stable at fluences well beyond the nodular ejection fluence.²⁶ Since these defects are quite small and benign nodular ejection pits tend to scatter less light than the original nodule, it is very possible that many of these most laser resistant mirrors may have damaged at lower fluence, but in such a benign way as not to be classified as laser damage by the detection methods utilized. On the other hand, nodular ejections from densified coatings from the different forms of sputtering may not eject until a higher fluence because they are more rigidly bounded. Therefore, the nodular ejections tend to be much more catastrophic and grow quickly with repeated laser irradiation. In fact the growth threshold for this damage morphology can be below the damage initiation fluence.²⁷

The most laser resistant 355 nm nanosecond pulse AR coatings were deposited by sol gel. The 193-nm excimer mirrors were deposited by RH because that is the easiest method to deposit metal fluoride coatings due to their low melting or sublimation temperature, although metal fluoride films have also been grown by IAD.²⁸ The chemical hazards associated with fluorine gas, which would be needed to grow fluoride coatings with sputtering technologies, have prevented widespread process development, although some interesting coating development has been done with this technology for the ultraviolet.²⁹ The most laser resistant short pulse HR coatings were all fabricated with sputtering technologies. For the broadband HR coating, densified coating processes such as sputtering, deposit materials with higher refractive indices than those deposited with lower energetic processes such as e-beam.³⁰ This increase in refractive index allowed a two-material design of HfO₂ and SiO₂, the best performing

material pair for most of the competitions, to meet the GDD specification, whereas e-beam deposited coatings needed to utilize a material with a higher refractive index than HfO₂ to meet the GDD specification. Sputtered coatings also tend to have superior bulk-like properties with lower scatter and absorption than e-beam deposited coatings. It has been proposed that short pulse coatings, which are less influenced by macroscopic defects, tend to have greater laser resistance for sputtered coatings with smaller defects that are more intrinsic in nature.

The 355-nm nanosecond pulse HR coating from the 2017 competition falls in an interesting process space. Much of the early laser damage work in this area was devoted to metal fluoride coatings due to their large bandgap; however, these materials tend to be tensile stressed, so these materials tend to craze for mirrors at this wavelength, which are almost twice the layer thickness of the excimer mirrors submitted in 2011. In this early laser damage work, IAD was proposed to decrease the tensile stress while maintaining high laser resistance.³¹ In the 355 nm nanosecond HR competition, no metal fluoride samples were submitted and the most laser resistant coating was deposited by IBS. One begs to ask the question, for the 355-nm nanosecond HR competition, does the higher photon energy of a UV coating favor more bulk-like thin film properties like short pulse coatings, particularly because the thickness of these films is one third that of the 1064 nm coatings, which leads to coatings with film thicknesses that may be too thin to mechanically hold onto micron scale nodular defects?

6 Impact of Polarization, Pulse Length, and Wavelength

For three of these competitions, samples were retested at either a different polarization (Brewster angle thin film polarizer) or a different pulse length (Fabry–Perot filter and broadband short pulse mirror). Also, in this series of competitions, high reflector mirrors have been fabricated for different spectral wavelengths ranging from 193 to 1064 nm. Some basic laser resistance trends emerge for thin films for the parameters of polarization, pulse length, and wavelength.

Brewster angle thin film polarizers are intentionally designed to maximize the polarizing splitting characteristics

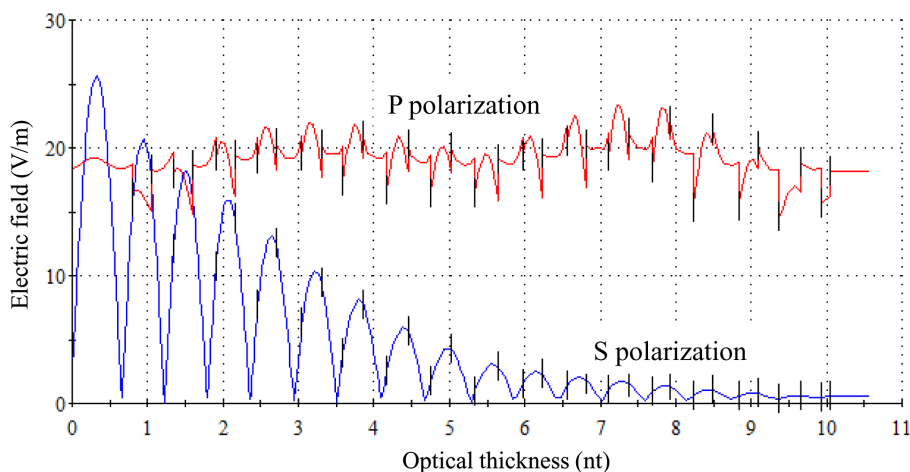


Fig. 7 Polarization-dependent standing-wave electric field profile of a typical long-wave-pass Brewster angle thin film polarizer. From left to right, the light propagates from the incident medium (air), through the multilayer stack, and into the Bk7 substrate.

of these optics. At S polarization, they are high reflectors, and at P polarization, they have high transmission. Additionally, as illustrated in Fig. 7, the standing-wave electric field profile is radically different for the two different polarizations. In P polarization, the standing-wave electric field magnitude remains high throughout the coating stack, whereas in S polarization, the standing-wave electric field magnitude quickly decays through the coating stack like a typical high reflector. Damage morphology differences have been reported with deep pitting for P polarization irradiation and shallow pitting at S polarization consistent with the polarization dependent electric field profiles.³² Attempts to broaden the polarization regime³³ or the use of a Fabry-Perot design³⁴ have also been reported to manufacture high laser damage threshold polarizers.

Despite the radically different standing-wave electric field profiles, the results of the competition showed for some samples similar laser resistance, as illustrated in Fig. 8. The laser resistance polarization difference for the sample with the highest S polarized damage threshold (42.6 J/cm²) was only 18% higher than the sample with the highest P polarized damage threshold (36.1 J/cm²). However, when evaluating the entire population average, there is a 43% higher average laser damage threshold difference between S polarization (24.4 J/cm²) and P polarization (16.8 J/cm²).

The ordering of the results in Fig. 8 is from lowest to highest S polarization laser resistance for each of the three different deposition techniques. Interestingly, there was no strong correlation between the best performing polarizers for the different polarizations. None of the most laser resistant samples from each deposition process at S polarization were the most laser resistant samples for each deposition process at P polarization. This result points to either spatially

nonuniform laser resistance across the samples or a different laser damage mechanism for the two different polarizations.

With regard to pulse length scaling, for transparent materials a typical thermal diffusion-based pulse length scaling relationship yielding a $\tau^{1/2}$ dependence (τ = pulse length) exists for pulse widths greater than 10 ps.^{35,36} For thin films, this scaling relationship has been slightly modified to fit experimental data and attributed to macroscale coating defects. A strong deviation from the $\tau^{1/2}$ dependence is observed below 10 ps, indicating a transition between an ablative regime (<10 ps) and a thermal regime (>10 ps).^{37,38} Attempts to identify pulse length scaling relationships that

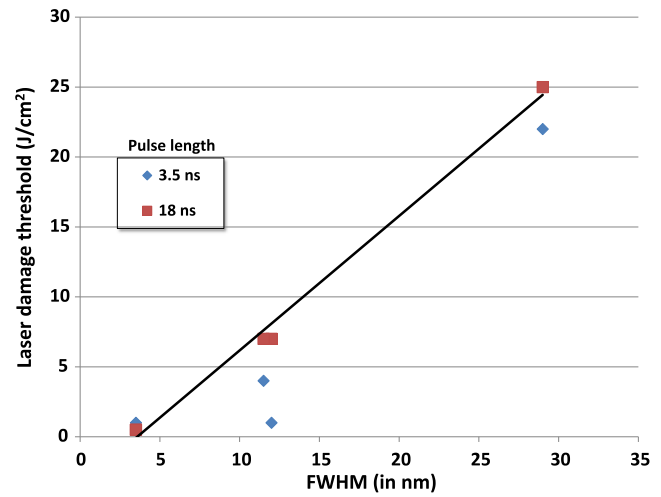


Fig. 9 Linear relationship between laser resistance and transmission spectral bandwidth has a stronger dependence at longer pulse length.

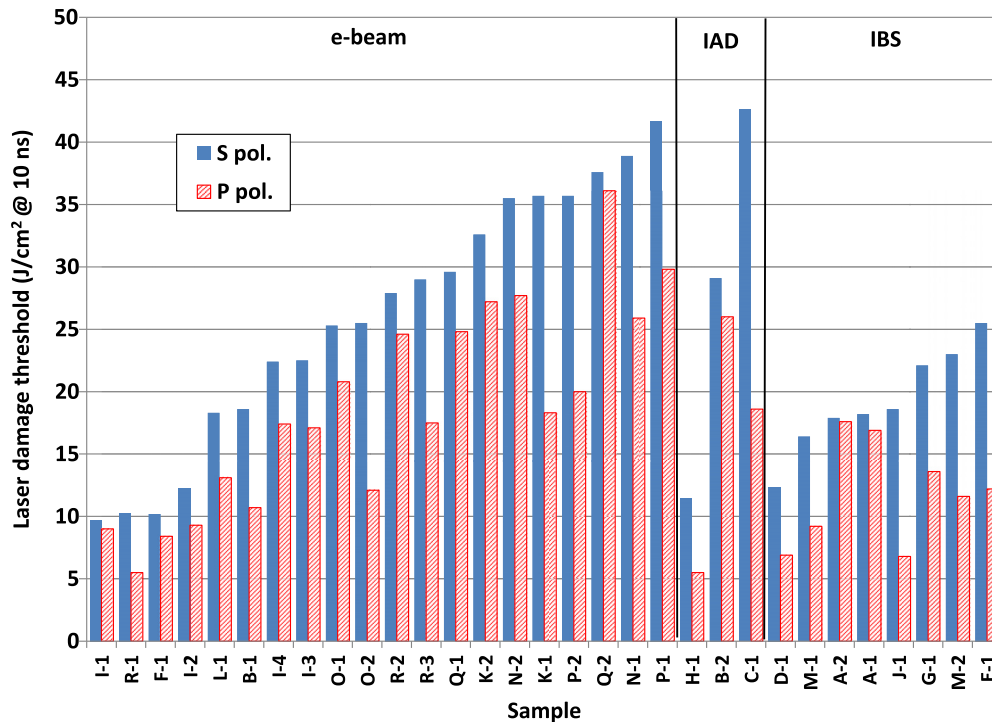


Fig. 8 Comparison between S and P polarization laser damage resistance for Brewster angle thin film plate polarizers as a function of participant and deposition process.

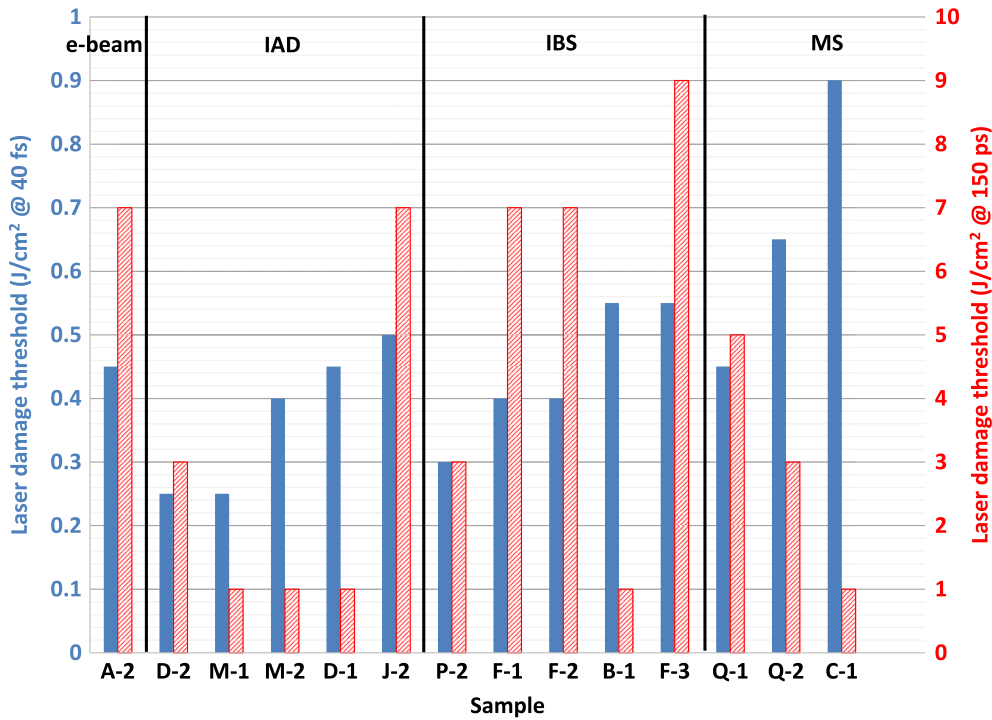


Fig. 10 Comparison between 40-fs and 150-ps pulse length laser damage resistance for a broadband high reflector with GDD of 100 fs² as a function of participant and deposition process.

match experimental data for thin films have shown significant deviations from theory.³⁹

In this series of laser damage competitions, there have been two instances where the impact of pulse length on laser damage threshold have been performed, the Fabry-Perot filter in 2014 and the broadband short pulse mirror in 2015 and 2016, as illustrated in Figs. 9 and 10,

respectively. For the broadband short pulse mirror, a wide range of pulse lengths was investigated (40 fs and 150 ps) over multiple deposition technologies. It is clearly observed in Fig. 10 that there is no correlation between the highest laser damage threshold coatings tested at 40 fs and the highest laser damage threshold coatings at 150 ps. Because the transition between ablative and thermal damage mechanisms

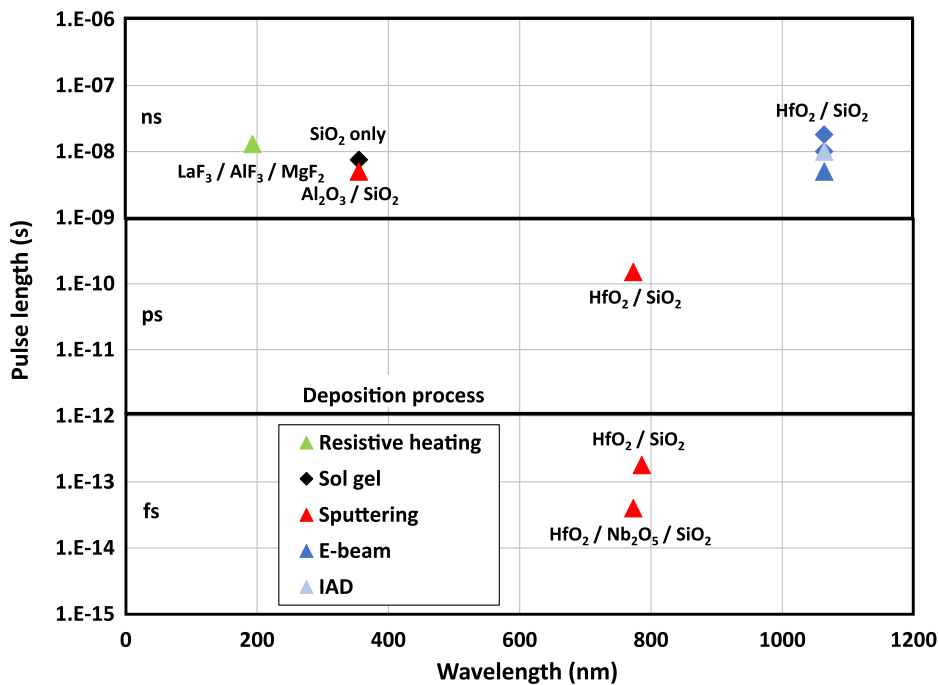


Fig. 11 Summary of the winning entries of each competition as a function of wavelength, pulse length, deposition process, and coating material reveal optimum coating materials are wavelength dependent and the optimum deposition processes are pulse length dependent.

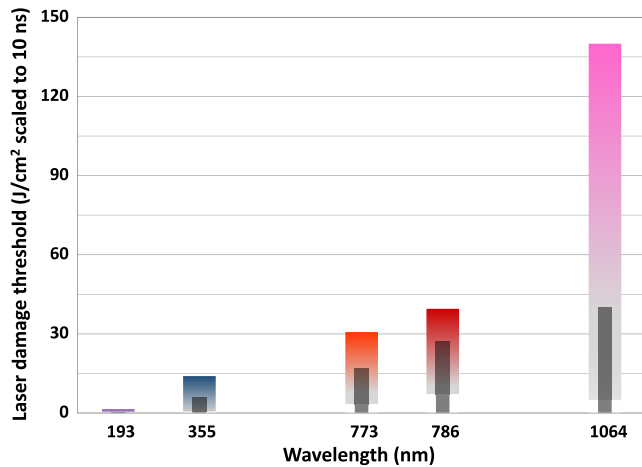


Fig. 12 Damage threshold range (colored bars) and median value (gray bars) for high reflectors increase with higher wavelength. The results are all scaled to 10 ns using a scaling factor of $\tau = 0.35$.

occurs between these two pulse lengths, this result is not completely surprising. These results do suggest an interesting hypothesis that film properties optimized for one pulse length may not necessarily have a positive impact at a significantly different pulse length. Alternately stated, the impact of coating defects on the laser damage threshold of a coating may differ significantly depending on the pulse length.

A summary of the impact of the wavelength, pulse length, deposition process, and coating material for the highest threshold entries of each competition is shown in Fig. 11. A few general trends emerge. In the near-infrared, regardless of pulse length, the optimum coating materials are hafnia and silica. For short wavelength coatings, wide bandgap materials perform best. Densified coating processes (sputtering) have the best laser resistance for short pulse coatings in the femtosecond and picosecond regime. For nanosecond pulses, porous coatings (e-beam, RH, and sol gel) perform best independent of wavelength. The 3ω high reflector competition was an exception since the best performing samples were deposited by IBS, a densified coating process. Future damage competitions of short pulse coatings at short wavelengths will help clarify whether optimum materials are pulse length independent and whether densified coatings perform better at short pulses.

A summary of the impact of wavelength on the damage threshold of high reflector coatings is illustrated in Fig. 12. Because the damage testing was performed over a wide range of different pulse lengths over the history of this series of competitions, the laser damage thresholds were scaled to 10 ns. A general trend that was observed from this data is that the laser damage threshold increased for high reflector coatings with increasing wavelength. Additionally, the range or spread in laser damage threshold for the contributed samples increased dramatically with wavelength.

7 Conclusions

The results of this series of damage test competitions show that a wide range of laser damage threshold exists for coatings within the optical coating industry. Femtosecond and excimer coatings tended to have a smaller damage threshold range most likely due to the more intrinsic behavior at short

pulse lengths and short wavelengths. Alternatively, damage thresholds for 1064-nm mirrors and 351-nm antireflection coatings illuminated with nanosecond length pulses tend to have a significant variation in damage threshold indicating more stochastic defect driven damage mechanisms. Coating materials and deposition method typically have a significant impact on the laser resistance of optical coatings with increased bandgap materials performing better as the laser wavelength is decreased. As the laser pulse length decreases, the optimum deposition process transitions from low energetic processes yielding porous coatings to increasingly energetic processes, and hence, more densified coatings. Finally, poor laser damage threshold correlations between samples tested at different polarizations or pulse lengths suggest different laser damage mechanisms between these two different conditions.

Acknowledgments

The authors would like to acknowledge all of the participants who prepared the samples over the last 10 years and provided the information about how the coatings were manufactured. These samples represent a significant investment to manufacture by the companies that participated. Spica, LZH, Quantel, and the OSU have each graciously donated their laser damage testing services with rapid turnaround of the results for these damage competitions. KMLabs graciously donated the GDD measurements for the 2015 and 2016 broadband short pulse mirror competitions. Organization of the laser damage testing results and samples was also performed by multiple administrative assistants over the years, including Jenessa Dozhier, Artika Lal, Terri Goodwin, and Heather Thomas. This work was performed under the auspices of the U.S. Department of Energy by Lawrence Livermore National Laboratory under Contract DE-AC52-07NA27344, IM #940723.

References

1. C. J. Stolz, M. D. Thomas, and A. J. Griffin, "BDS thin film damage competition," *Proc. SPIE* **7132**, 71320C (2009).
2. C. J. Stolz et al., "Thin film femtosecond laser damage competition," *Proc. SPIE* **7504**, 75040S (2010).
3. C. J. Stolz et al., "BDS thin film UV antireflection laser damage competition," *Proc. SPIE* **7842**, 784206 (2010).
4. C. J. Stolz et al., "Excimer mirror thin film laser damage competition," *Proc. SPIE* **8190**, 819007 (2011).
5. C. J. Stolz and J. Runkel, "Brewster angle polarizing beamsplitter laser damage competition: 'P' polarization," *Proc. SPIE* **8530**, 85300M (2012).
6. C. J. Stolz and J. Runkel, "Brewster angle polarizing beamsplitter laser damage competition: 'S' polarization," *Proc. SPIE* **8885**, 888509 (2013).
7. C. J. Stolz et al., "1064-nm Fabry-Perot transmission filter laser damage competition," *Proc. SPIE* **9237**, 92370N (2014).
8. C. J. Stolz et al., "150-ps broadband low dispersion mirror thin film damage competition," *Proc. SPIE* **9632**, 96320C (2015).
9. R. A. Negres et al., "40-fs broadband low dispersion mirror thin film damage competition," *Proc. SPIE* **10014**, 100140E (2016).
10. R. A. Negres et al., "355-nm, nanosecond laser mirror thin film damage competition," *Proc. SPIE* **10447**, 104470X (2017).
11. <http://www.spicatech.com/> (27 November 2018).
12. <https://www.lzh.de/en/departments/lasercomponents> (27 November 2018).
13. <http://www.quantel-laser.com/en/laser-damage-test-services.html> (27 November 2018).
14. <https://u.osu.edu/chowdhury.24/> (27 November 2018).
15. <https://www.kmlabs.com/> (27 November 2018).
16. M. R. Borden et al., "Improved method for laser damage testing coated optics," *Proc. SPIE* **5991**, 59912A (2006).
17. ISO 21254-2:2011, "Lasers and laser-related equipment – Test methods for laser-induced damage threshold – Part 2: threshold determination."

18. ISO 11146-1:2005, "Lasers and laser-related equipment – Test methods for laser beam widths, divergence angles and beam propagation ratios – Part 1: Stigmatic and simple astigmatic beams."
19. C. J. Stolz et al., "A study of laser conditioning methods of hafnia silica multilayer mirrors," *Proc. SPIE* **3578**, 144–152 (1999).
20. W. Stöber, A. Fink, and E. Bohn, "Controlled growth of monodisperse silica spheres in the micron size range," *J. Colloid Interf. Sci.* **26**, 62–69 (1968).
21. I. M. Thomas, "High laser damage threshold porous silica antireflective coating," *Appl. Opt.* **25**, 1481–1483 (1986).
22. K. Robbie and M. J. Brett, "Sculptured thin films and glancing angle deposition: growth mechanics and applications," *J. Vac. Sci. Technol. A* **15**, 1460–1465 (1997).
23. T. I. Suratwala et al., "HF-based etching processes for improving laser damage resistance of fused silica optical surfaces," *J. Am. Ceram. Soc.* **94**(2), 416–428 (2011).
24. J. Menapace et al., "Combined advance finishing and UV laser conditioning process for producing damage resistant optics," U.S. Patent 6920765 (2005).
25. P. J. Martin et al., "Ion-beam-assisted deposition of thin films," *Appl. Opt.* **22**(1), 178–184 (1983).
26. M. R. Kozlowski et al., "Surface morphology of as-deposited and laser-damaged dielectric mirror coatings studied in-situ by atomic force microscopy," *Proc. SPIE* **1556**, 68–78 (1992).
27. H. Ma et al., "Effect of boundary continuity on nanosecond laser damage of nodular defects in high-reflection coatings," *Opt. Lett.* **42**, 478–481 (2017).
28. U. J. Gibson and C. M. Kennemore III, "Ion-assisted deposition of MgF₂ at ambient temperatures," *Thin Solid Films* **124**, 27–33 (1985).
29. D. Ristau et al., "Ultraviolet optical and microstructural properties of MgF₂ and LaF₃ coatings deposited by ion-beam sputtering and boat and electron-beam evaporation," *Appl. Opt.* **41**(16), 3196–3204 (2002).
30. B. Pond et al., "Comparison of the optical properties of some high-index oxide films prepared by ion beam sputter deposition with those of electron beam evaporated films," in *Laser-Induced Damage in Optical Materials: 1986*, H. E. Bennett et al., Eds., NBS SP 752, pp. 410–417 (1987).
31. T. Izawa et al., "Damage threshold of fluoride HR coatings at 352 nm," *Proc. SPIE* **1848**, 322–329 (1999).
32. J. Zhang et al., "Broadband thin-film polarizers for high-power laser systems," *Appl. Opt.* **52**, 1512–1516 (2013).
33. M. Zhu et al., "Theoretical and experimental research on spectral performance and laser-induced damage of Brewster's thin film polarizers," *Appl. Surf. Sci.* **257**(15), 6884–6888 (2011).
34. U. B. Schallenberg and N. Kaiser, "Damage-resistant thin film plate polarizer," *Proc. SPIE* **2966**, 243–249 (1997).
35. E. S. Bliss, "Pulse duration dependence of laser damage mechanisms," *Opto-Electronics* **3**, 99–108 (1971).
36. E. S. Bliss, D. Milam, and R. A. Bradbury, "Dielectric mirror damage by laser radiation over a range of pulse durations and beam radii," *Appl. Opt.* **12**, 677–689 (1973).
37. M. J. Soileau et al., "Temporal dependence of laser-induced breakdown in NaCl and SiO₂," in *Laser-Induced Damage in Optical Materials: 1982*, H. E. Bennett et al., Eds., NBS SP 669, pp. 387–405 (1983).
38. B. C. Stuart et al., "Optical ablation by high-power short-pulse lasers," *J. Opt. Soc. Am. B* **13**, 459–468 (1996).
39. K. H. Guenther et al., "1.06 micron laser damage of thin film optical coatings— a round robin experiment involving various pulse lengths and beam diameters," in *Laser-Induced Damage in Optical Materials: 1983*, H. E. Bennett et al., Eds., NBS SP 688, pp. 241–267 (1984).

Christopher J. Stolz has been in the laser program at Lawrence Livermore National Laboratory (LLNL) since 1989, researching high-power laser coatings for the Atomic Vapor Laser Isotope Separation (AVLIS) laser and the National Ignition Facility (NIF). Currently, he manages the NIF Optics Production group. He is the founder of the international thin film damage competition held annually at the SPIE Laser Damage Symposium.

Raluca A. Negres has been a staff scientist at Lawrence Livermore National Laboratory (LLNL) since 2007. Her research interests include laser-matter interactions and optical materials characterization, time-resolved imaging, ultrafast laser systems and statistical modeling. Currently, she is serving on the program committee for the SPIE Laser Damage Symposium and is organizing the Thin Film Laser Damage Competition.